ISSN 0026-2617, Microbiology, 2011, Vol. 80, No. 3, pp. 420–431. © Pleiades Publishing, Ltd., 2011.
Original Russian Text © V.N. Danilevich, E.A. Vasilenko, E.V. Pechnikova, O.S. Sokolova, EV. Grishin, 2011, published in Mikrobiologiya, 2011, Vol. 80, No. 3, pp. 411–423.

EXPERIMENTAL ARTICLES

Micro- and Nanoparticles of Condensed DNA Formed in PCR with *Taq* Polymerase and Plasmid DNA as a Template

V. N. Danilevich[a, 1], E. A. Vasilenko[a], E. V. Pechnikova[b], O. S. Sokolova[b], and E. V. Grishin[a]

[a] *Shemyakin and Ovchinnikov Institute of Bioorganic Chemistry, Russian Academy of Sciences, Moscow, Russia*

[b] *Shubnikov Institute of Crystallography, Russian Academy of Sciences, Moscow, Russia*

Received June 22, 2010

Abstract—Formation of micro- and nanoparticles of condensed DNA during PCR with microbial genomic DNA or plasmid DNA as templates was reported previously. Initially, the microparticles were formed using a thermostable *KlenTaq* polymerase, which is a deletion variant of *Taq* polymerase. The present work shows that *Taq* polymerase is also capable of efficient formation of micro- and nanoparticles of condensed DNA in PCR. Electron microscopy revealed a number of morphological types (more than four) of microparticles produced in PCR with different reaction buffers in the presence of *Taq* polymerase and different plasmid DNAs as a template. In the case of some kinds of amplicons, an increase in the number of thermal cycles was shown to result in production of numerous nanowires and electron-dense spherical nanoparticles. The PCR conditions for preferential formation of discs (or ellipsoids) a few micrometers in diameter and several dozens of nanometers in thickness were determined. The structure of microparticles formed in the presence of *Taq* polymerase was found to depend on the level of synthesis of single-stranded DNA fragments in PCR. Experiments with nuclease S1 revealed that, along with double-stranded DNAs of the amplicon, micro- and nanoparticles contained single-stranded DNA fragments, which were absolutely necessary for their formation. In light of these data, the molecular mechanism of micro- and nanoparticle formation in the course of PCR is discussed.

Keywords: polymerase chain reaction (PCR), *Taq* polymerase, *KlenTaq* polymerase, DNA condensation, microparticles and nanoparticles of condensed DNA, epifluorescence microscopy, electron microscopy.

DOI: 10.1134/S0026261711030088

DNA is known to be present in viruses and cells in the form of compact aggregates of high density, that is, in a condensed form. The density of DNA packing in the condensed state is several orders of magnitude higher than that in solution. A number of studies have been devoted to the problem of DNA condensation. DNA condensation in vitro is a good model for investigation of the mechanisms of DNA condensation in live systems. Studying these mechanisms is important for understanding the molecular mechanisms of regulation of such biological processes as replication and transcription.

Condensation of double-stranded DNA in vitro at room temperature may be induced by various ligands, in particular, polyamines (spermine, spermidine) [1, 2] or cations of three-valent metals, for example, by cobalt–hexamine ($Co(NH_3)_6^{+++}$) [3–7]. Earlier, it was shown that Mg^{2+} cations in aqueous solutions were unable to induce condensation of double-stranded DNA [8] and even induced the reverse process of DNA decondensation [4]. At the same time, Mg^{2+} and other bivalent cations may act as condensing agents in solutions with low dielectric constants, for example, in water–alcohol mixtures [7]. The mechanism of ligand-induced DNA condensation is presently well studied [9–11].

We have previously described the phenomenon of condensed DNA (micro- and nanoparticles) formation during polymerase chain reaction (PCR) [12–14]. Micro- and nanoparticles are formed during the latest stages of PCR using gene-specific and/or incompletely complementary oligonucleotide primers with genome DNA of microorganisms or plasmid DNA molecules as templates.

Initially, we used mainly *KlenTaq* polymerase to obtain microparticles. This enzyme is a deletion mutant of *Taq* polymerase comprising 832 amino acid residues [15]. *KlenTaq* polymerase lacks the N-terminal fragment of 235 amino acid residues determining the 5'⟶3' exonuclease activity of the enzyme [16]. *KlenTaq* polymerase is more precise in terms of template copying than *Taq* polymerase [16].

DNA microparticles formed during PCR are rather stable in water [13, 14]. They are, however, easily destroyed (dissociated) in the presence of low amounts of EDTA (1 mM) [13, 14]. The major dissociation product is a linear double-stranded DNA flanked by

[1] Corresponding author; e-mail: dan@mx.ibch.ru

the primers sefences (that is, the DNA amplicon). The fact of microsphere destruction in the presence of EDTA indicates the importance of Mg^{2+} cations contained in the PCR buffer for the microsphere formation and structure stabilization. Moreover, the presence of metal cations (Mg^{2+} and K^{+}) in microparticles determines their ability to adsorb electrons, making it possible to visualize these structures by means of electron microscopy without the use of uranyl acetate as a contrasting agent.

The microparticles of condensed DNA formed during PCR possess a number of characteristic features, in particular, unique morphology and ultrastructural organization. Thus, microparticles obtained in PCR on yeast genomic DNA using *KlenTaq* polymerase were electron-dense microspheres with numerous spikes and ~1 μm in diameter [13]. If plasmid DNA was used as a template, large microspheres (about 3 μm in diameter) of several morphotypes, as well as aggregates of microspheres, were formed in PCR with *KlenTaq* polymerase [14]. If bacterial genome DNA was used as a template for PCR with *KlenTaq* polymerase, microspheres heterogeneous in size with diameters ranging between 1 and 7 μm were formed [14]. However, the most important peculiarity of the microparticles formed during PCR is that they contain both double-stranded (amplicon) and single-stranded DNAs [17]. The role of the latter ones in microsphere formation is still to be elucidated.

Preliminary studies demonstrated that *Taq* polymerase is significantly less efficient in terms of microparticle formation than *KlenTaq* polymerase, although the principal possibility of accumulating microparticles in PCR using *Taq* polymerase was demonstrated [14].

The goal of the present work was to explore the conditions and patterns of micro- and nanoparticle formation in the course of PCR on plasmid templates in the presence of a thermostable *Taq* polymerase, to study their structure (ultrastructure) by electron microscopy, and to determine the role of single-stranded DNA fragments in the process of micro- and nanoparticle formation.

MATERIALS AND METHODS

Template DNA samples. Plasmid DNA preparations were obtained using a Wizard reagent kit (Promega, United States) according to the manufacturer's protocol. Plasmids pBS::IST2, pBS::ISAfe1, and pBS::ISAfe600, are derivatives of pBlueScriptIIsk+, with in corporated insertion elements IST2, ISAfe1, and ISAfe600 from *Acidithiobacillus ferrooxidans* were used in the work. Their sizes were 1400, 1250, and 600 bp, respectively [18]. Plasmid DNA samples (about 500 ng/ml) were diluted 200-fold in distilled water, and 1-μl aliquots of the dilutions were used per 50 μl of the PCR mixture.

PCR procedure. PCR amplification of the IS fragments was carried out with the E1.1f + E1.2r and E2.1f + E2.2r primers [14]. PCR buffers, as well as the PCR cycling mode and primer oligonucleotide sequences, were reported earlier [14]. Linear double-stranded DNAs, PCR products, as well as plasmid DNAs, were analyzed by electrophoresis in 0.8–1.0% agarose gel [19].

The procedure of DNA isolation and purification was described in detail previously [13].

Staining of DNA microparticles with fluorescent dyes and fluorescent microscopy of the samples. Microparticles obtained in PCR were stained with DNA-intercalating fluorescent dyes, usually with propidium iodide (PI). The staining procedure was described earlier [13]. After incubation with PI, PCR mixtures were treated under standard conditions and the sediments of condensed DNA were resuspended in distilled water. Microparticle samples were studied under an Olympus CK40 (Germany) epifluorescence microscope. The details were reported previously [13].

Electron microscopy of the total samples of DNA nano- and microparticles was performed on a Tecnai G^2 spirit twin microscope (FEI Company, Netherlands) equipped with a digital Block Mega View III camera. For sample preparation, 5-μl aliquots of microparticle aqueous suspensions were applied to copper grids with pioloform supports and dried at room temperature to complete removal of water. The samples were viewed at the accelerating voltage of 120 kV.

Microparticle treatment with DNA nuclease S1. Nuclease S1 (Fermentas, Lithuania) solution of 100 AU/μl was used in the work. Eight microliters of 5× buffer for nuclease S1 and 2 μl of the 100-fold diluted enzyme (2 AU) were added to 30 μl of a DNA solution or microsphere aqueous suspension; total mixture volume was 40 μl. The microparticles were incubated with the nuclease for 1 h at 37°C. The reaction was terminated by addition of distilled water (200 μl). Then, the tubes were centrifuged at 12 000 rpm in an Eppendorf centrifuge for 75 s. The pellets were washed with water (200 μl) and at the final stage resuspended in 30–40 μl distilled water. Aliquots of the reaction mixture (5 μl) were used for light and electron microscopy.

RESULTS

Formation of superlarge microparticles in the presence of *Taq* polymerase (results of early experiments). In the first series of experiments, PCR amplification of the three IS elements was performed over 30 cycles.

As follows from the electrophoresis data, all samples after PCR contained DNA fragments matching the corresponding DNA amplicons in size (fragments of 1250, 600, and 1400 bp, respectively). Background fluorescence was of moderate intensity. In all three variants, huge (superlarge) microparticles were

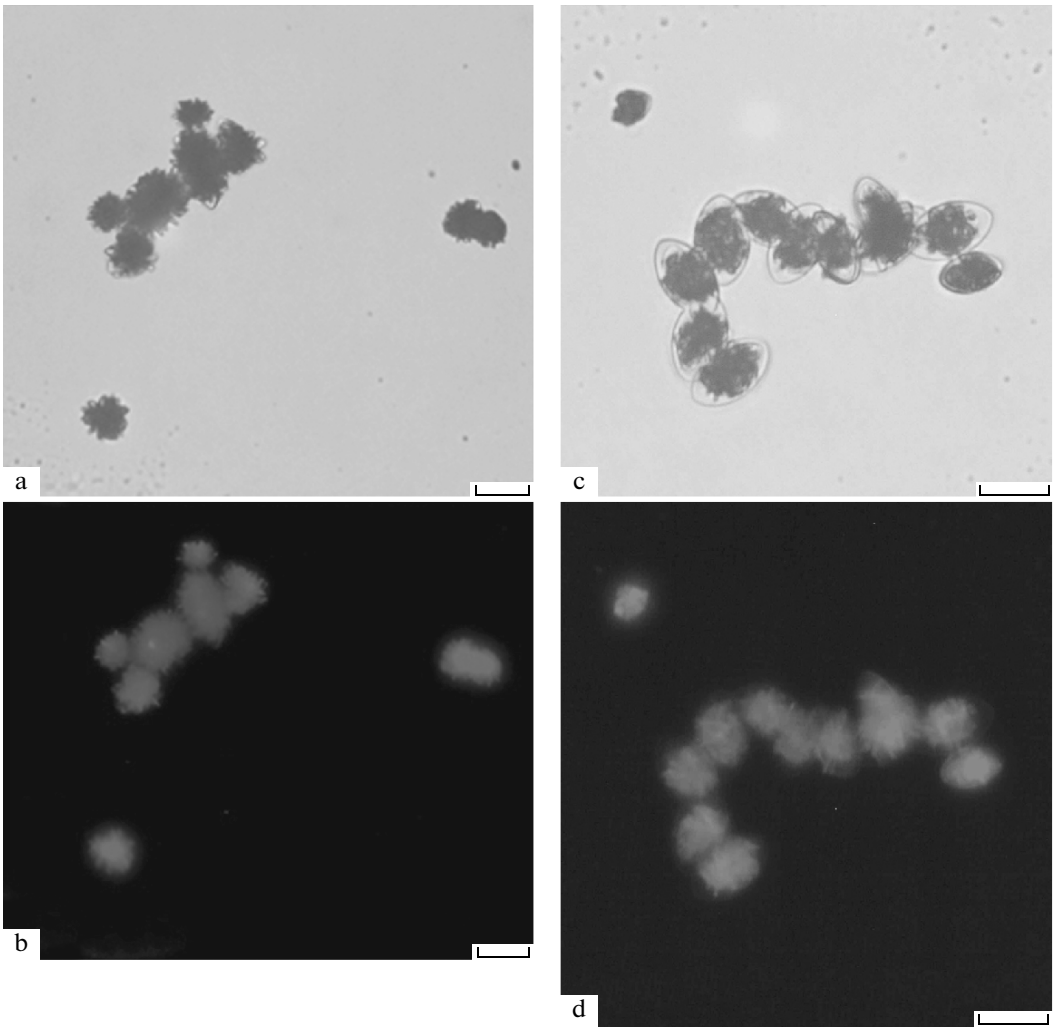

Fig. 1. Individual superlarge microparticles and aggregates of fused microparticles formed in PCR amplification (30 cycles) of the ISAfe1 (a) and (b) and IST2 (c) and (d) elements with *Taq* polymerase. In pictures (c) and (d), the microparticles are surrounded by fluorescent semi-transparent spheres. The microparticles are stained with PI. The images are in transmitted white light (a) and (c) and fluorescence in the red region of the spectrum (b) and (d). Scale bar length is 20 μm.

revealed by fluorescence microscope of PI-stained samples. Microparticles were observed both in white light and under excitation with green light, resulting in red fluorescence (Fig. 1). The microparticles were 10–20 μm in diameter. The number of microparticles in the samples was extremely low, a little over 100 per 50 μl of the PCR mixture. Apart from individual microparticles, numerous aggregates, some of them bizarre in shape, were observed (Fig. 1). Microparticle edges were limbate with projections. The fluorescence of the microparticles obtained with *Taq* polymerase was several times lower than that of the particles obtained with *KlenTaq* polymerase with the same primers and templates [14]. In many cases there was a glowing sphere of unclear origin around the microparticles (Fig. 1B). Microparticles of this kind were not studied.

Formation of condensed DNA microparticles in PCR with *Taq* polymerase (results of further experiments). The above-presented data prove that *Taq* polymerase is indeed less efficient than *KlenTaq* in terms of microparticle formation [14]. The reason for this could be the difference in the working buffer composition for *KlenTaq* and *Taq* polymerases. However, lately we demonstrated that microparticle formation with *Taq* polymerase was rather efficient in two different buffers used for the reactive mixture, that is, the potassium chloride buffer usually applied for PCR with *KlenTaq* polymerase and the standard *Taq* polymerase ammonium sulfate buffer. In the experiment, PCR amplification of the ISAfe1 and IST2 sequences was performed with *Taq* polymerase and corresponding primers. An electrophoresis picture of the linear DNA products of the PCR is presented in Fig. 2.

It should be noted that, according to electrophoresis data, the PCR products obtained in two different buffers showed no significant differences. In both variants, double-stranded DNA fragments of 1250 and 1400 bp were formed and background fluorescence was negligible although noticeable. The length of DNA fragments matched the size of the ISAfe1 and IST2 elements. Centrifugation of the PCR mixtures revealed sediments perceptible to the naked eye. The standard washing procedure yielded microparticle suspensions in water. They were studied with optical and electron microscopy (EM).

Electron microscopy of the microparticles produced in potassium chloride buffer. Epifluorescence microscopy of the microparticles produced in PCR amplification of IST2 element using *Taq* polymerase in KCl buffer showed that most microparticles were individual, while some formed aggregates of from two or three up to eight particles. The number of aggregates produced by *Taq* polymerase was considerably lower than that with *KlenTaq* polymerase. The samples were studied in more detail by electron microscopy.

Electron micrographs of the microparticles produced in PCR amplification of the ISAfe1 element are presented on Fig. 3. Microparticles of several morphotypes were revealed in the samples. Type I microparticles were large (3–7 μm in diameter), cone-shaped, and electron-dense (Fig. 3a). Type II microparticles were elliptical in shape, with major and minor axes of 3–4 and 2 μm, respectively (Fig. 3b). Since the electron density of the ellipses varied, the most probable 3D view of these particles is a flattened ellipsoid of varying thickness. A considerable share of the particles was assigned to an intermediate type III, microparticles of spherical or close to spherical shape with small projections and/or spines. Finally, type IV was represented by infrequent ellipsoid microparticles with sharp extended spines and axes of 5 and 2.5 μm. Large cone-shaped particles and particles of the intermediate type were predominant in the studied samples.

Electron micrographs of the microparticles obtained in PCR amplification of the IST2 element in KCl buffer are presented on Figs. 3c–3e. While the microparticle dimensions differed insignificantly from those described above, much more particles with sharp thorns were present in this sample. On Fig. 3d, semi-electron-dense ellipses rarely occurring in the sample are shown (type II microparticles). Their 3D view is that of flattened ellipsoids of equal or similar thickness of about 100 nm according to our estimations. We have previously observed and characterized similar structures in other experiments [20]. Special attention should be drawn to type IV microparticles (Fig. 3d). In addition to the sharp spines, the particles also contain semitransparent projections, apparently resulting from superimposed microparticles of type II, semitransparent ellipses, at different angles. A closeup view of the microparticles of the intermediate type III (smooth microspheres with several spines) is presented on Fig. 3e. The size of the microparticles obtained in PCR amplification of the ISAfe1 and IST2 elements in KCl buffer using *Taq* polymerase was generally slightly higher (up to 1.5 times) than that of the microparticles formed with *KlenTaq* polymerase [20].

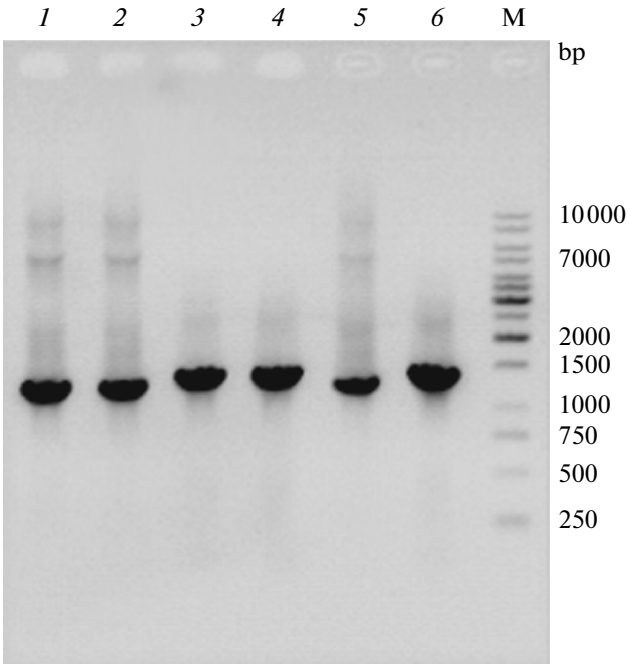

Fig. 2. Agarose gel electrophoresis picture of the products of PCR amplification of the ISAfe1 (*1*, *2*, *5*) and IST2 (*3*, *4*, *6*) elements with *Taq* polymerase. Two buffer systems were used, potassium chloride buffer (*1–4*) and ammonium sulfate buffer (*5* and *6*). M is the DNA molecular weight marker (1 kb DNA ladder).

Characterization of the microparticles obtained in ammonium sulfate buffer. The microparticles obtained by amplification of the ISAfe1 and IST2 elements in ammonium sulfate buffer was studied subsequently.

Light microscopy showed that most microparticles obtained by PCR amplification of ISAfe1 formed aggregates of from two to three up to ten or more particles. Some aggregates were linear and branched, while some were compact. Few individual microparticles were observed. Light microscopic analysis revealed several types of microparticles differing by size, morphology, and density. Microparticle size varied between 2–3 and 10 μm. At the same time, in the samples obtained during PCR amplification of IST2 under the same conditions, mainly individual particles were present (data not shown).

Electron microscopy demonstrated that, in general, the microparticles formed using the ammonium sulfate buffer (Figs. 4 and 5) were similar to those obtained in the potassium chloride buffer, although considerably larger than the latter ones. Some microparticles were up to 10 μm along the small axis and 15 μm, along the major one. Several morphotypes were

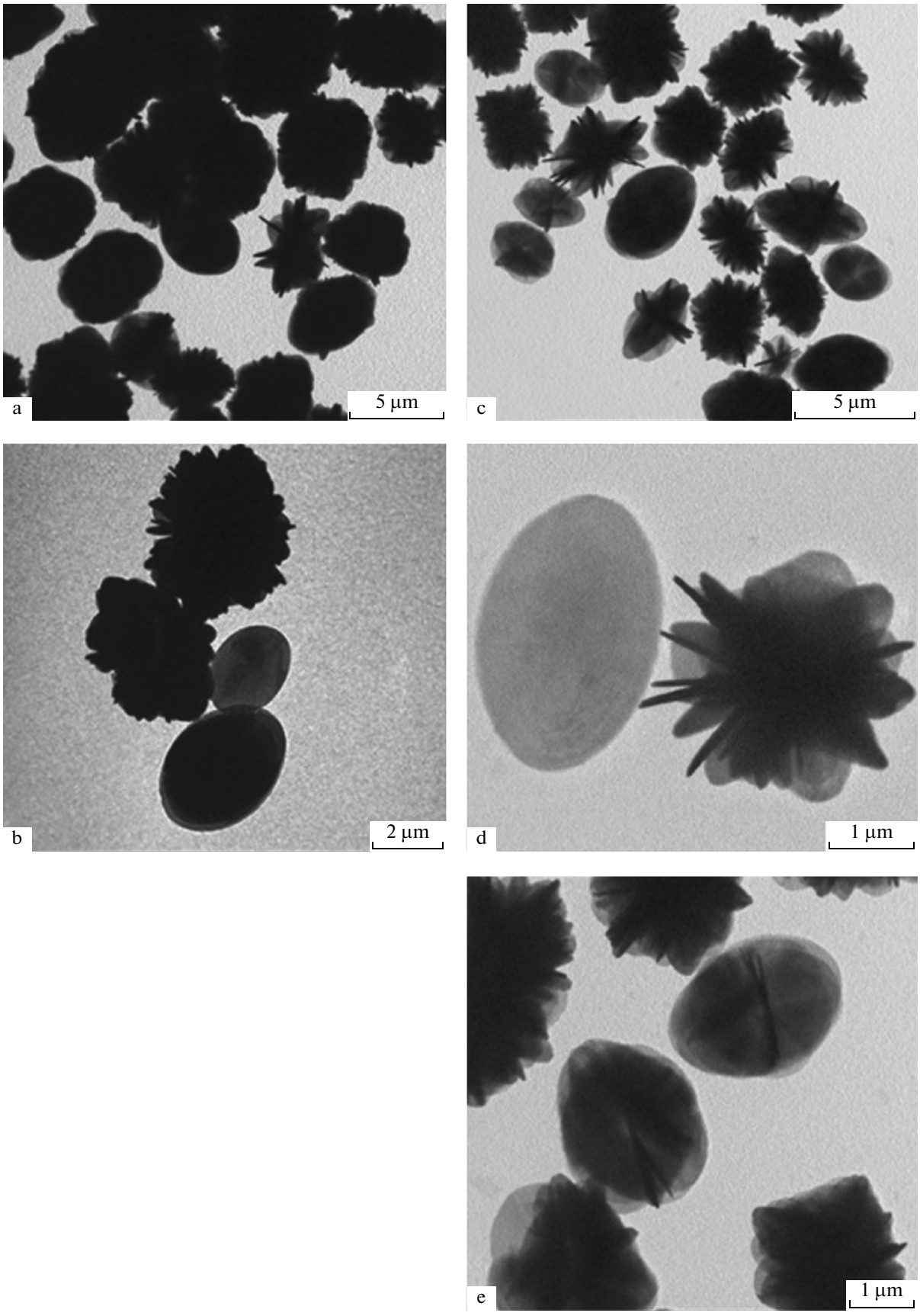
a
5 μm
c
5 μm
b
2 μm
d
1 μm
e
1 μm

Fig. 3. Electron microscopic (EM) images of microparticles obtained in PCR amplification of the ISAfe1 (a) and (b) and IST2 (c), (d), and (e) elements with *Taq* polymerase in potassium chloride buffer. Cluster of microparticles (a); cone-shape microparticles, smooth ellipsoidal microparticles, and microparticles with extended projections (b); panoramic view of microparticles (c); semi-electron-dense microparticle in the shape of a flattened ellipsoid and a microparticle with sharp spines and semi-transparent projections (starlike) (d); and microparticles of an intermediate type—smooth microspheres with a single spine or several spines (e).

detected, including cone-, corolla-, star-, and butterfly-shaped particles.

Large electron-dense cone-shaped microparticles about 10–12 μm long with numerous spines and projections are shown in Figs. 4a and 5a; the periphery of the particles (area of the projections) is sometimes semi-electron-dense. Star-type microparticles with sharp protruding spines are also present on Fig. 4a.

Microparticles in the shape of a butterfly are presented on Fig. 5b. They consist of two parts (wings) with numerous sharp spines near the area where the wings join together. The length of the microparticles reaches 15 μm.

Another type of microparticles (Fig. 5c) is a corollalike flower made of several petals with some spines. Apparently, the individual petals are the semi-electron dense ellipses described above. The corolla is probably formed when several ellipses overlap under different angles, since, in the area of overlapping, as can be noticed at the periphery of a particle, the electron density increases. In addition to these individual microparticles, aggregates of joint microparticles were present. One of the aggregates is shown in Fig. 5d.

Thus, PCR with *Taq* polymerase yields microparticles somewhat different in morphology from those generated with *KlenTaq* polymerase [20]. Moreover, the microparticles obtained with *Taq* polymerase are larger. These results also suggest that the shape and size of the microparticles depend on the PCR buffer. Interestingly, in the samples under study, we did not observe three-dimensional networks similar to those formed in the presence of *KlenTaq* [20].

PCR with an increased number of cycles. Nanofilament growth conditions. As follows from the electron microscopy data, many samples of condensed DNA also contained long electron-absorbing threads, or nanofilaments. These structures were described previously [17, 20]. Few filaments were present in the samples under study, although, in some fields of the supporting grid, filament clusters were observed. Therefore, the next goal of our work was to study how the number of PCR cycles affected the spectrum of the resulting micro- and nanoparticles. An increase in the number of PCR cycles is well known to result in accumulation of DNA amplicon and exhaustion of deoxynucleoside triphosphates. Consequently, synthesis of full-size amplicons is slowed down sharply and the share of incomplete duplexes resulting from annealing of shortened single-stranded DNA fragments below the amplicon length increases.

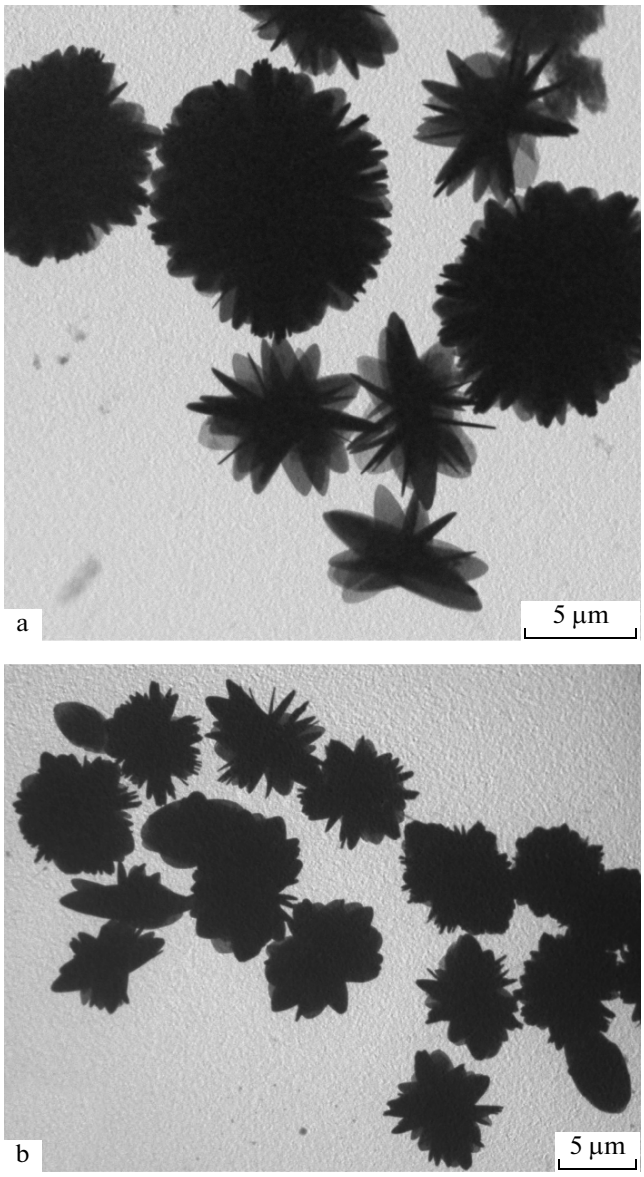

Fig. 4. EM images of the clusters of microparticles obtained in PCR amplification of the ISAfe1 (a) and IST2 (b) elements using *Taq* polymerase in ammonium sulfate buffer. In picture (a), two types of microparticles are shown—large cone-shaped ones and microparticles with sharp extended spines (starlike).

Under the experimental conditions described above (*Taq* polymerase in KCl buffer), the number of PCR cycles was increased from 30 to 35. The differences in the numbers and relative content of micro- and nanoparticles were studied.

In electrophoresis pictures of the samples obtained at 35 PCR cycles, the fluorescence intensity of the bands corresponding to the amplicon DNA increased slightly (about 1.5-fold) in comparison to 30 cycles.

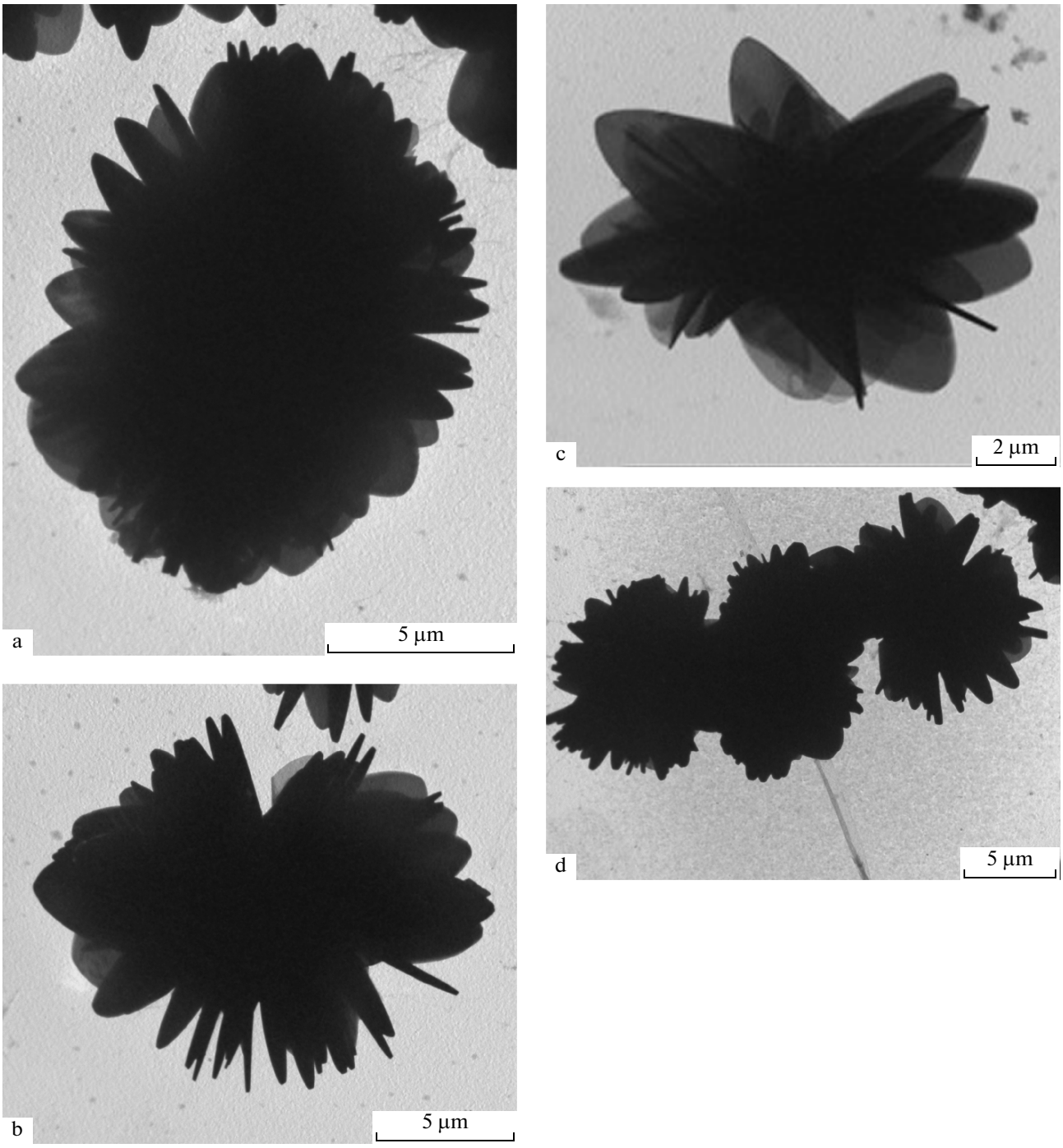

Fig. 5. EM images of individual microparticles obtained in PCR amplification of the ISAfe1 element using *Taq* polymerase in ammonium sulfate buffer. Large electron-dense cone-shaped microparticles (a), butterfly-shaped microparticles (b), flower corolla-shaped microparticles (c), and aggregate of three fused microparticles (d).

The sediment volume also increased slightly. Electron microscopy of the samples (30 and 35 cycles) revealed microparticles of four types, namely, smooth spherical, large cone-shaped, star-shaped, and intermediate. No significant difference in the size and morphology of the particles was registered with increase of the number of PCR cycles (data not shown); the particle titer increased slightly.

Along with the microparticles, nanofilaments were present in all samples. In the samples produced by the amplification of ISAfe1, nanofilaments were rather rare. The increase in the number of thermal cycles practically did not change the number of filaments.

A completely different picture was observed during amplification of the IST2 element. In the samples obtained at 30 PCR cycles, individual nanofilaments

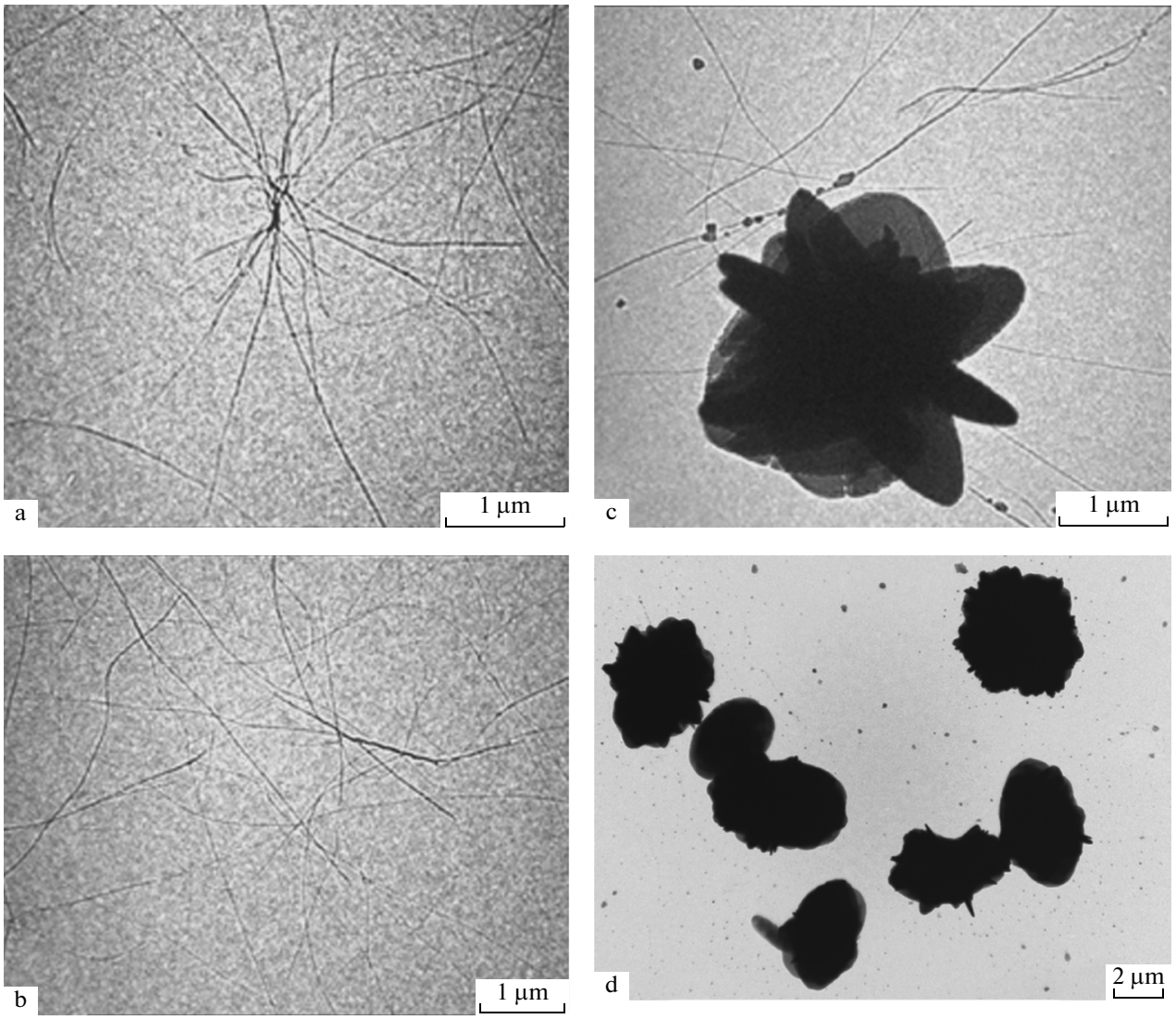

Fig. 6. EM images of clusters of nanofilaments and spherical nanoparticles. The samples were obtained in PCR amplification of the IST2 element using *Taq* polymerase during 35 (a), (b), and (d) or 30 cycles (c). In panel (c), the filaments are positioned close to the microparticles, electron-dense nanodots are associated with them. In panel (d), numerous spherical nanoparticles differing in size and electron density are situated near the microparticles.

were typically present, and the clusters were rare. After 35 cycles, a considerable increase (by more than two orders of magnitude) was observed in the number of both individual filaments and those assembled in bundles (Fig. 6).

These results evidence that the ability to accumulate nanofilaments in PCR depends on both the increase in the number of PCR cycles and the amplicon structure. The structural features of the DNA amplicon determining this ability are presently not clear.

Nanodots and other spherical nanoparticles formed in the presence of *Taq* polymerase. Investigation of the microparticles obtained during PCR amplification of the ISAfe1 and IST2 fragments with *Taq* polymerase revealed also nanodots and larger spherical nanoparticles. The term "nanodots" is used here to denote the smallest spherical nanoparticles (several dozen nanometers in size) observed under an electron microscope without uranyl acetate staining. Typically, spherical nanoparticles were rather rare. However, in some samples they were abundant.

Thus, in the samples obtained by PCR amplification of IST2 (30 cycles), in addition to microparticles and nanofilaments, we observed electron-dense spherical nanoparticles, some of them residing individually, while others were in close contact with the nanofilaments (Fig. 6c). Electron microscopy of the samples obtained in PCR with an increased number of cycles revealed an increase in the number of individual electron-dense spherical nanoparticles (Fig. 6d). The picture shows that electron density of the nanopar-

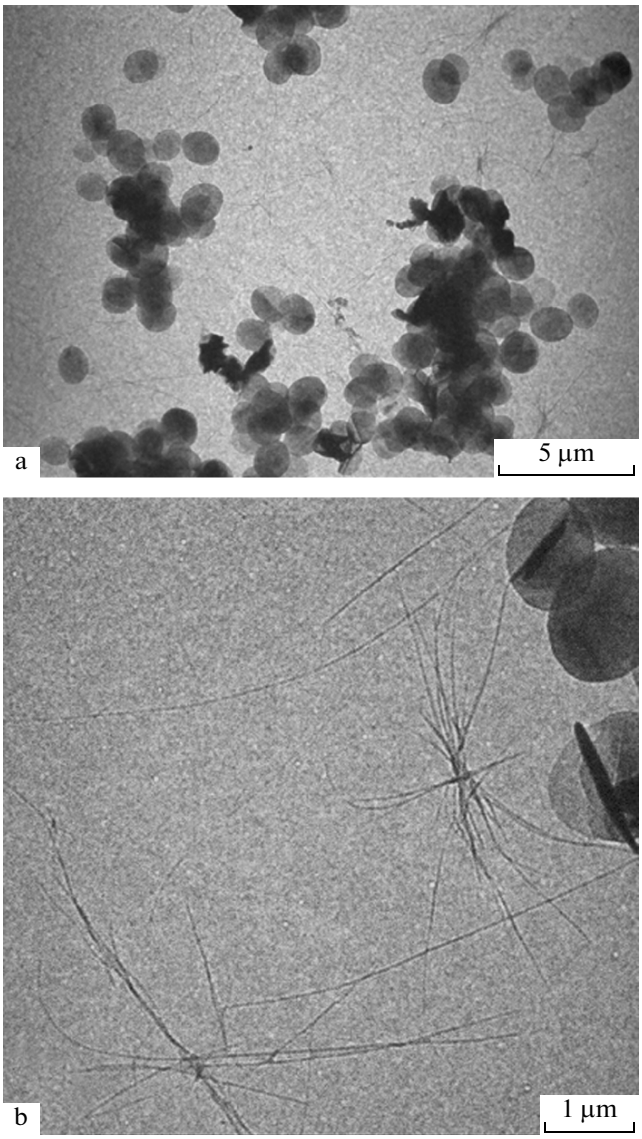

Fig. 7. EM images of microparticles obtained in PCR amplification of the IST2 element using *Taq* polymerase during 35 cycles (low-background experiment). Accumulation of ellipsoids and electron-dense microparticles (a) and bundles of nanofilaments near the ellipsoids (b).

ticles increased with their size—from dozens nanometers to 200 nm. Spherical nanoparticles were also present in abundance in samples obtained under different conditions, for example, during asymmetrical PCR (unpublished data).

Other types of microparticles formed in PCR with *Taq* polymerase. We tried to determine why, in our early experiments with *Taq* polymerase (for example, in the presence of yeast genomic DNA [13]), microparticles were absent, while PCR with *KlenTaq*, under the same conditions, led to accumulation of considerable amounts of microparticles. It could be suggested that the number, size, and morphology of microparticles in the PCR mixture depend on the amount of single-stranded DNA fragments produced in PCR along with the DNA amplicon. To test this hypothesis, PCR amplification of the IST2 element was performed using *Taq* polymerase under conditions excluding accumulation of nonspecific (background) products. For this purpose, freshly prepared solutions of the PCR mixture components (dNTPs and primers) were used. PCR was performed under standard conditions. No sediment of condensed DNA was formed upon centrifugation of the PCR mixtures obtained after 30 thermal cycles. After five additional cycles (total number of cycles 35), the sediment appeared.

As followed from the electrophoresis pictures of the PCR products, a rather large amount of DNA amplicon accumulated after 35 cycles, while background fluorescence was practically absent (data not shown). Electron microscopy revealed that the samples contained mainly small ellipse-shaped microparticles with a major axis length not exceeding 1.5 μm (Fig. 7). The number of microparticles in the samples was very large, over 1×10^7 per 50 μl of the PCR mixture. In most cases the particles were semi-electron-dense. In a 3D view, the particles were flattened ellipsoids about 100 nm thick according to AFM (unpublished data). It should be noted that the electron density varied within a single ellipse, indicating that the surface was not ideally flat. In the samples, some electron-dense microparticles differing in shape from ellipses were also present (Fig. 7). As is demonstrated by Fig. 7a, partial overlapping of two discs (thickness doubling) results in a sharp increase of electron density in the region of overlapping. Some of the revealed electron-dense microparticles were apparently formed upon aggregation of two or more ellipses.

Another peculiar feature of these samples was high filament content. Filaments were either scattered chaotically or accumulated in the form of bundles (Fig. 7b). The filaments were observed in practically each field of the supporting grid.

It should be noted that in the repeated experiment on PCR amplification of IST2 using *Taq* polymerase performed after a month with the same concentrated PCR reagent solutions the results were somewhat different. Large ellipses of about 4 μm accumulated and the microparticle titer was lower by an order of magnitude (data not shown).

Therefore, the morphology of the microparticles formed in PCR with *Taq* polymerase may be determined to a certain extent by the synthesis rate of the single-stranded DNA fragments. We do not exclude also the role of other, unrevealed, factors in microparticle morphogenesis.

Effect of nuclease S1 activity on DNA microparticles obtained with *Taq* polymerase. Earlier it was demonstrated that microparticles contained single-stranded DNA fragments synthesized in the course of PCR [17].

To confirm the presence of single-stranded DNA fragments in the microparticles under study, they were treated with S1 nuclease, which, under optimal conditions, cleaves single-stranded DNA fragments while ignoring the double-stranded DNA helices [17].

Prior to use, the S1 nuclease preparation (100 AU/μl) was diluted 100-fold in the working buffer and its activity was tested on the native double-stranded DNA and on the same DNA denatured by heating at 100°C. At the concentration of 1–2 AU per 20 μl of the reaction mixture, the nuclease cleaved exclusively the denatured DNA and did not affect the double-stranded one. On the basis of these data we treated the microparticles with the enzyme concentration of 2 or 4 AU per 40 μl of the reaction mixture.

In the experiment, fresh preparations of the microparticles obtained in PCR amplification of the IST2 element in KCl buffer under the standard conditions (30 cycles) were used. The morphotypes of the microparticles in these samples corresponded to those presented on Fig. 4. After incubation with S1 nuclease, the reaction mixtures were treated as described in the Materials and Methods section. The obtained suspensions were studied by electron microscopy.

It was found that 2 μl of enzyme per 40 μl of the reaction mixture was not enough for perceptible destruction of the microparticles, while a doubling of the enzyme concentration resulted in their complete destruction (Fig. 8). In the sample, after incubation with 4 μl of the enzyme, a huge amount of semitransparent "nanodots" was present, along with numerous spherical microparticles of medium and high electron density 0.2–0.4 μm in diameter (Fig. 8a) and cords of medium electron density (Fig. 8b). Within the ranges of these cords, clusters of large and medium spherical, electron-dense nanoparticles were localized. Some nanoparticles were located separately from the cords. We assume that the observed cords are the products of incomplete cleavage of electron-dense microparticles and their aggregates by S1 nuclease.

Therefore, the studied micro- and nanoparticles contained fragments of single-stranded DNA.

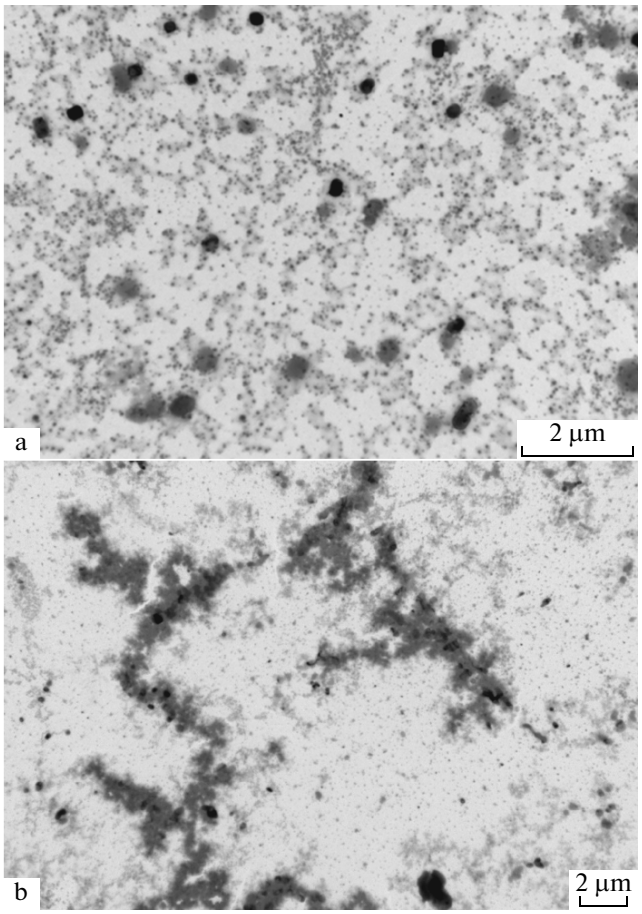

Fig. 8. EM images of the products of microparticle deep cleavage with S1 nuclease. The microparticle preparation was obtained in PCR amplification of the IST2 element using *Taq* polymerase. Panels (a) and (b) are different fields within the same supporting grid. Spherical nanoparticles of different electron density and size are observed together with the electron-dense cords.

DISCUSSION

It is known that ligands such as polyamines and trivalent cobalt ions induce condensation of double-stranded DNA in water solutions in vitro, resulting in the formation of a narrow spectrum of particle morphotypes, mainly toroids and rods of nanometer scale. Independently of DNA size, the toroid inner diameter is 400 Å and the outer is ~ 800 Å [2, 4]. On the contrary, DNA condensation in the course of PCR generates the widest spectrum of micro- and nanoparticles differing both by size and morphology.

Initially, microparticles were obtained in PCR using *KlenTaq* polymerase on yeast genomic DNA as a template [13]. In our next work [14], we found that usage of plasmid DNA templates in PCR result in formation of larger microparticles different in their morphology from those obtained with yeast genomic DNA.

Thus, in PCR with plasmid templates, microparticles of several types were formed in the presence of *KlenTaq*, namely, 1) spherical or ellipsoid in shape with a smooth surface, 2) of ellipsoid shape with extended large spines and/or conelike projections, and 3) of an intermediate kind [20]. So-called three-dimensional network structures of irregular shape were also present in the PCR mixtures of this kind [20].

In the present work, we found that another enzyme, *Taq* polymerase, is also capable of efficient micro- and nanoparticle generation. In the PCR mixtures obtained in the course of standard PCR amplifications of ISAfe1 and IST2 elements with *Taq* polymerase, several microparticle morphotypes were distinguished, that is, 1) large cone-shaped, 2) with extended sharp spines (star-shaped), 3) smooth ellipsoidal, and 4) of an intermediate kind. It should be

noted that the microparticles obtained with *Taq* polymerase in KCl or ammonium sulfate buffer were 1.5 and 2–3 times larger, respectively, than those obtained with *KlenTaq* and the same templates.

Studying the effect of the PCR conditions on the amount and composition of the DNA condensation product revealed the possibility of accumulating a large amount of nanofilaments. Thus, in the presence of *Taq* polymerase and with the number of cycles of PCR amplification of IST2 increased to 35, the amount of nanofilaments was two to three orders of magnitude higher than at 30 amplification cycles. However, PCR amplification of another amplicon, ISAfe1, under the same conditions was not accompanied by an increase in nanofilament amount. Most probably, the formation of nanofilaments is governed not only by the conditions of the reaction, i.e., the PCR cycle number, but also by the amplicon structure. An increased number of PCR cycles led also to the emergence of large amounts of nanodots and larger spherical nanoparticles in the PCR mixture.

What are nanodots and other compact nanoparticles? Recently, we detected tiny disc-shaped nanoparticles about 10 nm in diameter and 1 or 2 nm thick (unpublished data). Apparently, these are elementary nanoparticles formed as a result of intramolecular Mg^{2+}-dependent condensation (compactization) of individual single- and double-stranded DNA molecules. AFM data also suggest that the nanodots and larger spherical nanoparticles observed in the EM experiments are aggregates comprising dozens of elementary nanoparticles or more.

Nanofilaments are formed according to a different mechanism than are nanodots, as a result of Mg^{2+}-mediated lateral condensation of several DNA helices. In other words, the filaments are bundles of several (up to ten) parallel DNA helices. The role of Mg^{2+} cations is to neutralize the negative charge of the phosphate groups and thus to decrease the electrostatic repulsion between DNA molecules required for their lateral condensation [4], as well as for the generation of compact three-dimensional nanoparticles.

We also showed the possibility of the formation of semi-electron-dense microparticles with micrometer-scale diameters and nanometer thicknesses that were discs or ellipsoids during PCR. These structures may also be considered as nanoparticles. Regular-shaped discs were generated in abundance in the course of asymmetric PCR with *Taq* polymerase (unpublished data). As for ellipsoids, they were accumulated in a routine PCR amplification of IST2 with *Taq* polymerase under the conditions of low rates of synthesis of nonspecific (single-stranded) DNA fragments. In this case, the yield of individual ellipsoids could reach 80% of the total microparticle number.

Therefore, in the presence of *Taq* polymerase under the same conditions and PCR cycling mode, condensed DNA particles of various morphologies may be formed. In one case they were microparticles of four morphotypes; in the other, ellipsoids. It is not always possible to predict the microparticles' morphotype in each PCR experiment with *Taq* polymerase. We assume that the morphology of the PCR-generated microparticles is determined to a considerable extent by the rate of single-stranded DNA fragment synthesis. Indeed, ellipsoid formation during IST2 amplification with *Taq* polymerase occurred only when the level of background fluorescence (the indicator of accumulation of single-stranded DNA fragments) upon electrophoresis was rather low. On the contrary, in the case of high background fluorescence level, the standard set of large electron-dense microparticles was formed. We do not exclude the influence of some other factors still to be revealed.

As for the internal structure of the discs (ellipsoids) of micrometer diameter and nanometer thickness, according to AFM data, they consist of numerous tightly packed spherical nanoparticles formed by double- and single-stranded DNA molecules (unpublished data).

We found that the microparticles obtained in PCR using *KlenTaq* polymerase and yeast genomic DNA as a template were partially degraded in the presence of low concentrations of S1 nuclease [17]. The microspheres became spongy, so that the individual structural elements (blocks) comprising the microparticles could be seen. These are particles of nanometer size: nanopatches of various shapes, nanodots, and nanoparticles of other topologies [17].

In the experiments with S1 nuclease, we proved that the microparticles obtained on plasmid templates with *Taq* polymerase also contain single-stranded DNA fragments. After treatment with S1 nuclease, rather deep cleavage of the microparticles down to nanoparticles was observed. It is still not clear whether these nanoparticles are the terminal products of nuclease cleavage or not.

Earlier, it was demonstrated that the presence of Mg^{2+} cations is insufficient for DNA condensation [8]. In independent model experiments, we found that, in the absence of a thermostable DNA polymerase, neither linear DNA fragments nor the supercoiled plasmid DNA are capable of condensation in the process of thermal cycling even in the presence of Mg^{2+} cations (unpublished data). This implies that along with Mg^{2+} cations, single-stranded DNA fragments are absolutely necessary for the condensation of double-stranded DNA amplicon and formation of micro- and nanoparticles. This conclusion is important for better understanding of the molecular mechanisms of DNA condensation during PCR. Investigation of micro- and nanoparticles of condensed DNA formed in the course of PCR will be continued.

ACKNOWLEDGMENTS

The work was supported by a grant of the Russian Foundation for Basic Research, project no. 10-08-00184-a.

REFERENCES

1. Gosule, L.C. and Schellman, J.A., Compact Form of DNA Induced by Spermidine, *Nature*, 1976, vol. 259, pp. 333–335.
2. Chattoraj, D.K., Gosule, L.C., and Schellman, J.A., DNA Condensation with Polyamines. II. Electron Microscopic Studies, *J. Mol. Biol.,* 1978, vol. 121, pp. 327–337.
3. Wilson, R.W. and Bloomfield, V.A., Counterion-Induced Condensation of Deoxyribonucleic Acid. A Light-Scattering Study, *Biochemistry,* 1979, vol. 18, pp. 2192–2196.
4. Widom, J. and Baldwin, R.L., Cation-Induced Toroidal Condensation of DNA: Studies with $Co_3(NH_3)_6$, *J. Mol. Biol.*, 1980, vol. 144, pp. 431–453.
5. Plum, G.E., Arscott, P.G., and Bloomfield, V.A., Condensation of DNA by Trivalent Cations. 2. Effects of Cation Structure, *Biopolymers,* 1990, vol. 30, pp. 631–43.
6. Arscott, P.G., Li, A.Z., and Bloomfield, V.A., Condensation of DNA by Trivalent Cations. 1. Effects of DNA Length and Topology on the Size and Shape of Condensed Particles, *Biopolymers,* 1990, vol. 30, pp. 619–630.
7. Arscott, P.G., Ma, S., Wenner, J.R., and Bloomfield, V.A., DNA Condensation by Cobalt Hexaamine (III) in Alcohol-Water Mixture, *Biopolymers,* 1995, vol. 36, pp. 345–364.
8. Ma, C. and Bloomfield, V.A., Condensation of Supercoiled DNA Induced by $MnCl_2$, *Biophys. J.*, 1994, vol. 67, pp. 1678–1681.
9. Bloomfied, V.A., Condensation of DNA by Multivalent Cations: Considerations on Mechanism, *Biopolymers,* 1991, vol. 31, pp. 1471–1481.
10. Teif, V.B., Ligand-Induced DNA Condensation: Choosing the Model, *Biophys. J.,* 2005, vol. 89, pp. 2574–2587.
11. Kornyshev, A.A. and Leikin, S., Electrostatic Interaction between Helical Macromolecules in Dense Aggregates: an Impetus for DNA Poly- and Meso-Morphism, *Proc. Natl. Acad. Sci. USA,* 1998, vol. 95, no. 23, pp. 13579–13584.
12. Danilevich, V.N., Petrovskaya, L.E., and Grishin, E.V., DNA Nano- and Microparticles: New Products of Polymerase Chain Reaction, *Doklady AN*, 2008, vol. 421, no. 1, pp. 119–122 [*Doklady Biochem. Biophys.*, vol. 421, pp. 168–170].
13. Danilevich, V.N., Barinova, E.S., and Grishin, E.V., Microparticles from Coupled DNA Formed in the Process of Polymerase Chain Reaction, *Bioorg. Khim.*, 2009, vol. 35, no. 2, pp. 226–238 [*Russ. J. Bioorg. Chem.* (Engl. Transl.), vol. 35, no. 2, pp. 207–218].
14. Danilevich, V.N. and Grishin, E.V., Characteristics of Microspheres Formed in PCR with Bacterial Genomic DNA or Plasmid DNA as Templates, *Mikrobiologiya*, 2009, vol. 78, no. 3, pp. 369–380 [*Microbiology* (Engl. Transl.), vol. 78, no. 3, pp. 328–338].
15. Lawyer, F.C., Stoffel, S., Saiki, R.K., Myambo, K., Drummond, R., and Gelfand, D.H., Isolation, Characterization, and Expression in *Escherichia coli* of the DNA Polymerase Gene from *Thermus aquaticus,* *J. Biol. Chem.,* 1989, vol. 264, no. 11, pp. 6427–6437.
16. Barnes, W.M., The Fidelity of *Taq* Polymerase Catalyzing PCR Is Improved by an N-Terminal Deletion, *Gene*, 1992, vol. 112, no. 1, pp. 29–35.
17. Danilevich, V.N., Kadykov, V.A., and Grishin, E.V., Micro- and Nanoparticles of Condensed DNA Formed in a PCR with Yeast Genomic DNA as a Template. Electron Microscopy Data, *Bioorg. Khim.*, 2010, vol. 36, no. 3, pp. 375–386 [*Russ. J. Bioorg. Chem.* (Engl. Transl.), vol. 36, no. 3, pp. 344–353].
18. Kondrat'eva, T.F., Danilevich, V.N., Ageeva, S.N., and Karavaiko, G.I., Identification of IS Elements in *Acidithiobacillus ferrooxidans* Strains Grown in a Medium with Ferrous Iron or Adapted to Elemental Sulfur, *Arch. Microbiol.*, 2005, vol. 183, pp. 401–410.
19. Maniatis, T., Fritsch, E.F., and Sambrook, J., Molecular Cloning: A Laboratory Manual, *Laboratory Press*, 1989, pp. 17–38.
20. Danilevich, V.N., Kadykov, V.A., and Grishin, E.V., Condensed DNA Particles Formed in a PCR with Plasmid Templates: An Electron Microscopy Study, *Bioorg. Khim.*, 2010, vol. 36, no. 4, pp. 535–546 [*Russ. J. Bioorg. Chem.* (Engl. Transl.), vol. 36, no. 4, pp. 497–507].